RESEARCH ARTICLE

EcoMat
FUNCTIONAL MATERIALS FOR GREEN ENERGY AND ENVIRONMENT

WILEY

Sustainable ultra-strong thermally conductive wood-based antibacterial structural materials with anti-corrosion and ultraviolet shielding

Haoran Ye[1] | **Yang Shi**[1] | **Ben Bin Xu**[2] | **Zhanhu Guo**[2] | **Wei Fan**[3] |
Zhongfeng Zhang[4] | **Daniel M. Mulvihill**[5] | **Xuehua Zhang**[6] | **Pengju Shi**[7] |
Ximin He[7] | **Shengbo Ge**[1]

[1]Co-Innovation Center of Efficient Processing and Utilization of Forest Resources, College of Materials Science and Engineering, Nanjing Forestry University, Nanjing, China

[2]Department of Mechanical and Construction Engineering, Northumbria University, Newcastle, UK

[3]School of Textile Science and Engineering & Key Laboratory of Functional Textile Material and Product of Ministry of Education, Xi'an Polytechnic University, Xi'an, China

[4]College of Furniture and Art Design, Central South University of Forestry and Technology, Changsha, China

[5]Materials and Manufacturing Research Group, James Watt School of Engineering, University of Glasgow, Glasgow, UK

[6]Department of Chemical and Materials Engineering, University of Alberta, Edmonton, Canada

[7]Department of Materials Science and Engineering, University of California, Los Angeles (UCLA), Los Angeles, California, USA

Correspondence
Ben Bin Xu, Department of Mechanical and Construction Engineering, Northumbria University, Newcastle Upon Tyne, NE1 8ST, UK.
Email: ben.xu@northumbria.ac.uk

Ximin He, Department of Materials Science and Engineering, University of California, Los Angeles (UCLA), Los Angeles, CA 90095, USA.
Email: ximinhe@ucla.edu

Shengbo Ge, Co-Innovation Center of Efficient Processing and Utilization of Forest Resources, College of Materials Science and Engineering, Nanjing Forestry University, Nanjing 210037, China.
Email: geshengbo@njfu.edu.cn

Funding information
Engineering and Physical Sciences Research Council, Grant/Award Number: EP/N007921; National Natural Science Foundation of China, Grant/Award Number: 32201491; China Postdoctoral Science Foundation, Grant/Award

Abstract

In light of the uprising global development on sustainability, an innovative and environmental friendly wood-based material derived from natural pinewood has been developed as a high-performance alternative to petrochemical-based materials. The wood-based functional material, named as BC-CaCl$_2$, is synthesized through the coordination of carboxyl groups (−COOH) present in pinewood with calcium ions (Ca^{2+}), which facilitates the formation of a high-density crosslinking structure through the combined action of intermolecular hydrogen bonds. The as-prepared BC-CaCl$_2$ exhibits excellent tensile strength (470.5 MPa) and flexural strength (539.5 MPa), establishing a robust structural basis for the materials. Meanwhile, BC-CaCl$_2$ shows good water resistance, thermal conductivity, thermal stability, UV resistance, corrosion resistance, and antibacterial properties. BC-CaCl$_2$ represents a viable alternative to petrochemical-based materials. Its potential application areas include waterproof enclosure structure of buildings, indoor underfloor heating, outdoor UV resistant protective cover, and anti-corrosion materials for installation engineering, and so forth.

KEYWORDS
coordination crosslink, excellent mechanical performance, ultra-strong, wood-based composite

1 | INTRODUCTION

Petrochemical energy serves as a vital component for industrial operations, playing a crucial role in human production and daily life.[1–3] Its products, derived from petroleum processing, includes gasoline, kerosene, diesel and various raw materials for polymer materials such as plastics, synthetic fibers, and synthetic rubber and so on.[4,5] These petroleum products have been widely used in various packaging and construction industries as a structural functional material.[6] However, the ever-increasing exploitation of oil as a non-renewable energy source will inevitably lead to energy depletion. Additionally, the diminishing availability of raw materials will necessitate a reduction in the production of petroleum-based materials.[7] Furthermore, the stable chemical properties of such materials make them difficult to degrade effectively.[8] Consequently, various waste materials derived from the petroleum-based products accumulate in the environment exerting great pressure on the environment.[9,10] Today, green development is a global consensus for sustainable growth. After the pandemic, many countries have adopted national policies with the primary goal of achieving "green recovery".[11] In this context, the development of bio-based materials utilizing biomass as raw materials has gained significant momentum,[12–15] positioning it as one of the most promising industries at present Moreover, the bio-based materials are poised to become a leading industry, driving scientific and technological innovation as well as economic development on the global scale.[16] Therefore, it is crucial to develop an all-green sustainable high-performance bio-based structural functional materials that rely solely on 100% biomass.[17,18]

Biomass is considered to be the main sustainable source of organic carbon on the earth,[19–24] a perfect equivalent to oil, and a sustainable green raw material for producing fuel and fine chemicals with net zero carbon emissions.[25–27] Meanwhile, bio-based composite materials are a new type of material that has emerged in recent years,[28–30] which refers to a new type of material that uses renewable biomass (such as crop straw fiber, bamboo and wood fiber, etc.) or materials made from biology as raw materials and is then compounded with other materials through biological, chemical, and physical methods.[31–34] Since the production of new building materials and building components is an indispensable link in the development of the modern construction industry, this marks a major change in the production method and represents a future development trend in the furniture and building materials industry.[35–37] Meanwhile, in the "Guiding Opinions of the General Office of the State Council on Promoting the Steady Growth of the Building Materials Industry" issued by the State Council of China, it is clearly proposed to "support the development of biomass building materials by using crop straw, bamboo fiber,[38] wood chips, and so forth, and develop biomass fiber reinforced wood plastic building materials and other products". Hence, the new biomass structural functional materials developed are the most original ecological synthetic environment-friendly materials, which conform to the direction of novel environment-friendly synthetic materials.[38–40] However, the biomass structural functional materials constructed so far either have poor mechanical properties or rely on the synthesis of petrochemical adhesives (phenol-formaldehyde resin or urea-formaldehyde resin).[41] These drawbacks will not only cause accelerated consumption of petrochemical energy, but also lead to serious environmental pollution and ecological damage. Therefore, it is of great significance to develop an advanced method to prepare new sustainable bio-based structural functional materials.[42,43]

As a traditional building material, wood has been widely used in ancient and modern architecture.[44–46]

As a kind of coniferous plant, pinewood is widely used in structural building materials and furniture products because of its low price, natural texture and long service life.[47] However, pinewood also has many defects. On one hand, it is soft and easy to crack and deform due to its high moisture content. On the other hand, the large amount of rosin in the pinewood will block its tracheid. It is often subject to degreasing treatment during use, which makes its processing complex.[48] Therefore, the high-value utilization rate of pinewood is not high. To combat this, high-temperature steaming or chemical treatment is usually used to reduce the resin content of wood. However, these methods can damage the structure of the pine itself. Hence, the extraction of pine resin by extraction has become a common treatment method for the high-value utilization of pinewood.

The performance of bio-based structural functional materials can be enhanced through the design of micronano structures.[49] Thereinto, Ca^{2+}, as a common metal ion, is usually cross-linked through coordination with $-COOH$, combining with high-density hydrogen bonds between cellulose microfibers and hemicellulose, to form a special high-density cross-linked network inside the wood. Under this treatment condition, the strength and dimensional stability of bio-based structural and functional materials are greatly enhanced, and they are endowed with multiple functions. Hence, aiming to make full use of pinewood to prepare high-performance and sustainable wood-based structural functional materials, a robust and effective method is reported in this study. The degreased pinewood is first chemically pretreated, then coordinated with $-COOH$ in the pinewood under the action of Ca^{2+}, and finally thermally molded into high-strength wood-based composite. The material shows remarkable mechanical properties, good dimensional stability, excellent thermal conductivity and outstanding UV resistance.[50] The excellent mechanical properties of BC-CaCl$_2$ provide a solid foundation for its application as a structural material in the building materials industry, such as anti-seismic buildings. In particular, pinewood is a fast-growing wood. The prepared high-performance wood-based composites address the inefficient use of pinewood and achieve the high-value utilization of natural wood. Therefore, this study complies with the ultimate strategy of global sustainable development. Meanwhile, the production process of this material is green and pollution-free, which meets the policy requirements of prioritizing ecological environment in socioeconomic development.[51] In addition, the material meets the requirement of excellent properties for a renewable and low-cost alternative to traditional petrochemical-based functional materials.[52] The potential application areas for BC-CaCl$_2$ include waterproof enclosure structure of buildings, indoor underfloor heating, outdoor UV resistant protective cover and anti-corrosion materials for installation engineering, and so forth.

2 | MATERIALS AND METHODS

2.1 | Raw materials and preparation of wood-based composites

The pinewood was purchased from Suqian Timber Wholesale Market in Jiangsu Province. After careful selection (from the same pinewood and free from cracks and growth defects), it was cut into wood chips of the same specification (length 50 mm, width 50 mm, thickness 5 mm). NaOH (96%), Na$_2$SO$_3$ (98%), and CaCl$_2$ (99%) were purchased from Shanghai Macklin Biochemical Co., Ltd., China.

Preparation of wood-based composites: First, the pine resin was fully removed from the cut pinewood chips by Soxhlet extraction (BC-E). Second, the extracted pine chips were immersed in the mixed aqueous solution of 2 M NaOH and 0.4 M Na$_2$SO$_3$ (solid-to-liquid ratio = 1:10), stirred and heated at 96°C for 4 h, rinsed with deionized water, and freeze-dried (BC-P). Next, the pretreated pinewood chips were immersed in CaCl$_2$ solution for 24 h in vacuum, rinsed with deionized water, and freeze-dried (BP-CaCl$_2$). Finally, the extracted, pretreated and impregnated pinewood chips were placed into the customized molds respectively (the dimensions of the slot: length 50 mm, width 50 mm), and the molds were pressed in a hot press machine (Dongguan Zhenggong Electromechanical Equipment Technology Co., Ltd., China) at a pressure of 45 MPa and a temperature of 180°C. After hot pressing for 1 h, the mold was cooled to room temperature and three kinds of the wood-based composites were taken out, named as: BC-E, BC-P, and BC-CaCl$_2$.

2.2 | Characterization

In each test, three samples were analyzed in parallel according to the requirements of GB/T 24511-2017. The density ρ of the prepared wood-based composites was calculated according to the formula $\rho = mass/volume$. The AGS-X universal mechanical testing machine (Shimadzu, Japan) was used to investigate the mechanical properties of the samples. Specifically, the test was performed on a sample of 50 mm × 6 mm × 3 mm at room temperature at a displacement rate of 1.5 mm/min. The lightness of the samples was measured with a colorimeter (SR60, Mitutoyo Precision Measuring Instrument Co., Ltd., Guangdong,

China). In the water resistance test, the prepared three samples were placed in water, and the changes of water absorption rate and water absorption thickness swelling rate were compared within 48 h. The DSA100S contact angle measuring instrument (KRUSS) was used to measure the contact angle of samples 2 μL of water was dropped onto the sample each time, and the contact angle was recorded within 10 s. Sulfuric acid (4 μL, 78%) (Nanjing Chemical Reagent Co., Ltd, China) was dropped on three samples respectively, and their corrosion resistance was analyzed by observing their surface states.

Thermal conductivity of the three samples was characterized by a thermal conductivity tester (DRPL-2B, Xiangtan Instrument Co., Ltd., China). In the case of continuous heating by the laser heater for 3 min, the samples were photographed and characterized by an infrared thermal imager (FLIR E5xt, FLIR, USA). The thermal stability of the samples were analyzed using a thermogravimetric analyzer (TA Instruments, TGA55 USA) at a heating rate of 20°C/min from room temperature to 640°C in a nitrogen atmosphere.

In the flame-retardant test, three samples were burned under an external flame of the alcohol lamp for 10 s. The burning conditions and final combustion conditions of the samples in different time periods were observed and compared. At 210°C, the samples were heated with acrylonitrile butadiene styrene (ABS), polyvinyl chloride (PVC), polypropylene (PP), polycarbonate (PC) and polyamide (PA) purchased from Chang'an Wald Plastic Products Factory in Guangdong, China, and their morphological changes were compared.

The ultraviolet visible (UV-Vis) spectrophotometer (UV1900, Shandong Qingdao Jingcheng Instrument Co., Ltd.) was used to characterize the UV transmittance of the samples. Quanta 200 scanning electron microscope (SEM, FEI, China) was used to characterize the cross-section morphology and energy dispersive spectra (EDS) of the samples.

The antibacterial performance of Escherichia coli was evaluated against a sample plate with a length and width of 2 cm × 2 cm.[53] The antibacterial properties of the samples were characterized according to the distribution range of Escherichia coli. Furthermore, this antibacterial experiment should be repeated 4 times.

2.3 | Chemical characterization

The National Renewable Energy Laboratory (NREL) method was used to determine the cellulose, hemicellulose, and lignin content in the samples. Functional groups of the samples were analyzed using VERTEX 80 V ATR Fourier infrared spectroscopy (FT-IR, Bruker Technology Co., Ltd., Germany). X-ray diffraction (XRD, Beijing Puwei General Instrument Co., Ltd., China) was performed in the scanning range of 5 to 60° (2θ) to analyze the diffraction patterns. X-ray photoelectron spectroscopy (XPS, Shimadsu Enterprise Management Co., Ltd., China) was used to investigate the elemental composition and molecular structure of the samples. The ^{13}C-NMR spectra of the samples were tested by high-resolution solid-state nuclear magnetic resonance spectroscopy (NMR, Bruker 400 M, Germany).

3 | RESULTS AND DISCUSSION

3.1 | Preparation of wood-based composites

Figure 1 shows the preparation process of high-strength wood-based composites. After most of the pine resin inside the extracted pinewood chips is removed to form a loose and porous structure, we obtain the raw material denoted as BC-E (Figure 1A). After chemical pretreatment with NaOH and Na_2SO_3, the sulfonation reaction occurs that etches the pinewood chips to remove part of the lignin (Figure S1A), and the raw material of BC-P is obtained.[54] Under vacuum-assisted conditions, the pretreated pinewood chips are fully immersed in the $CaCl_2$ solution to obtain the BC-$CaCl_2$ raw material. Finally, the three raw materials are pressed into regular plates with stable morphology by one-step hot molding.[55]

During the thermoforming process, part of the lignin seeps out of the plates in the molten state, and covers the surface of the material after cooling, forming a dense protective layer. The prepared high-performance wood-based structural functional material BC-$CaCl_2$.[56] The black surface of BC-$CaCl_2$ verifies that lignin covers the surface of the materials. The BC-$CaCl_2$ exhibits better density, mechanical properties, thermal conductivity, UV resistance, and water stability than BC-E and BC-P (Figure 1B). Especially, BC $CaCl_2$ shows excellent mechanical strength, indicating that under the action of Ca^{2+}, the treated pinewood produces a stable cross-linked structure. Meanwhile, BC-$CaCl_2$ is green and pollution-free, which enables its usage in building materials to replace the traditional petrochemical-based structural materials.[57]

3.2 | Chemical mechanism of preparation of BC-$CaCl_2$

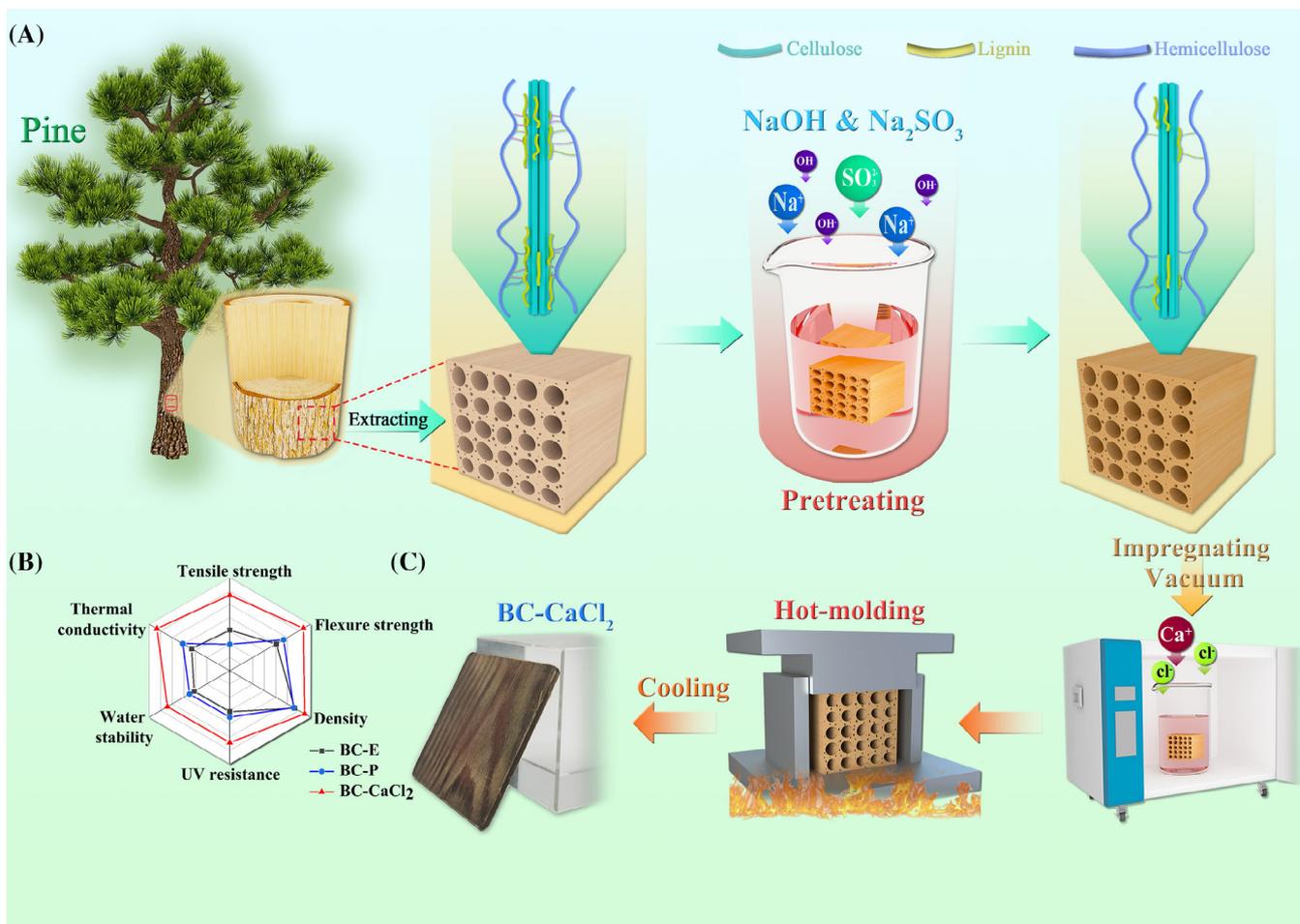Figure 2 reveals the strengthening mechanism of Ca^{2+} on the internal molecular structure of pretreated

FIGURE 1 (A) Schematic diagram of the preparation process of high-strength wood-based composites. (B) The density, mechanical property, thermal conductivity, UV resistance and water stability of BC-E, BC-P, and BC-CaCl$_2$.
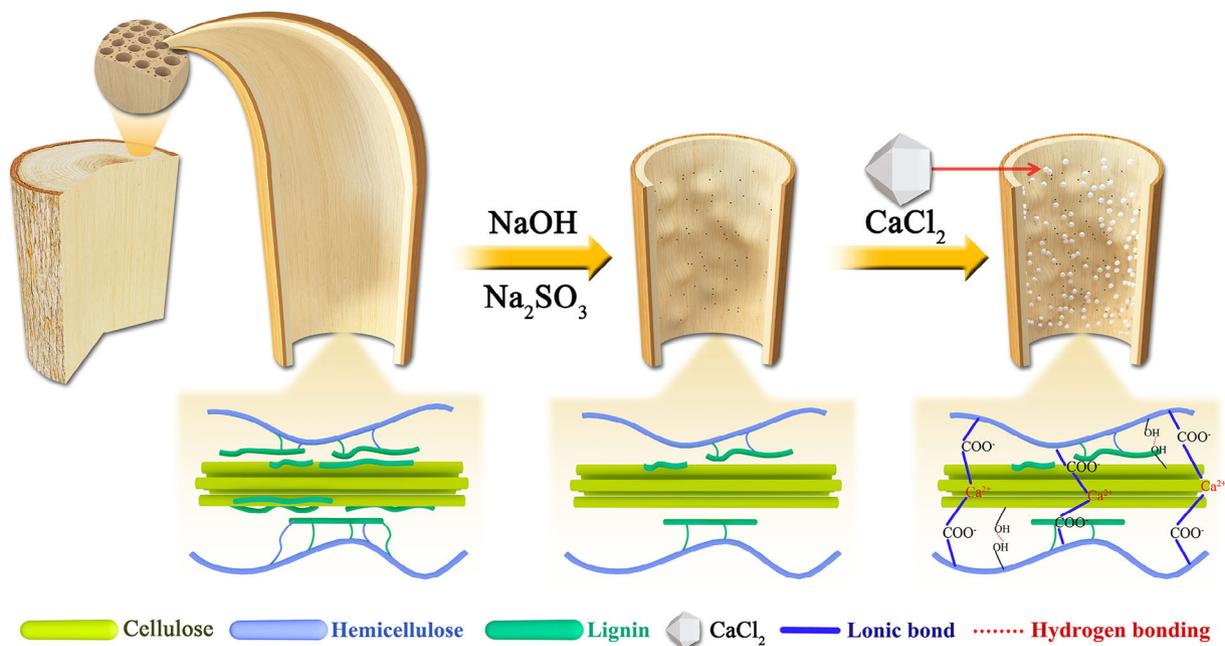

FIGURE 2 Schematic diagram of chemical mechanism of BC-CaCl$_2$.

pinewood. First, most of the pine resin has been removed from the extracted pinewood, making it loose and porous, showing a well-defined cross-linked structure of cellulose, hemicellulose and lignin. Then, the internal structure of the pinewood is etched under the treatment of an alkaline solution, removing part of the lignin to expose the internal cellulose microfiber and hemicellulose structure. Finally, under the action of Ca^{2+}, a special high-density cross-linked structure can be formed with pinewood, including high-density hydrogen bonding between cellulose microfiber and hemicellulose, and coordination crosslinks between Ca^{2+} and $-COOH$. This high-density cross-linked structure can enhance the structural stability and strength of BC-$CaCl_2$, and improve its hydrolysis resistance and durability.[50,58]

Meanwhile, the presence of Ca^{2+} endows BC-$CaCl_2$ with certain antibacterial properties.

3.3 | Chemical properties of BC-CaCl2

Under vacuum impregnation of $CaCl_2$ solution, the white crystalline building blocks in BC-$CaCl_2$ are composed of the cross-linked structure formed by $-COOH$ in hemicellulose and Ca^{2+} (Figure 3A).[59] Figure 3B,C shows the general distribution of C and Ca elements. Meanwhile, Figure 3D shows the mass percentage distribution of Ca element. Therefore, EDS composition analysis shows that BC-$CaCl_2$ contains a high concentration of Ca atoms, which further proves the strong binding between
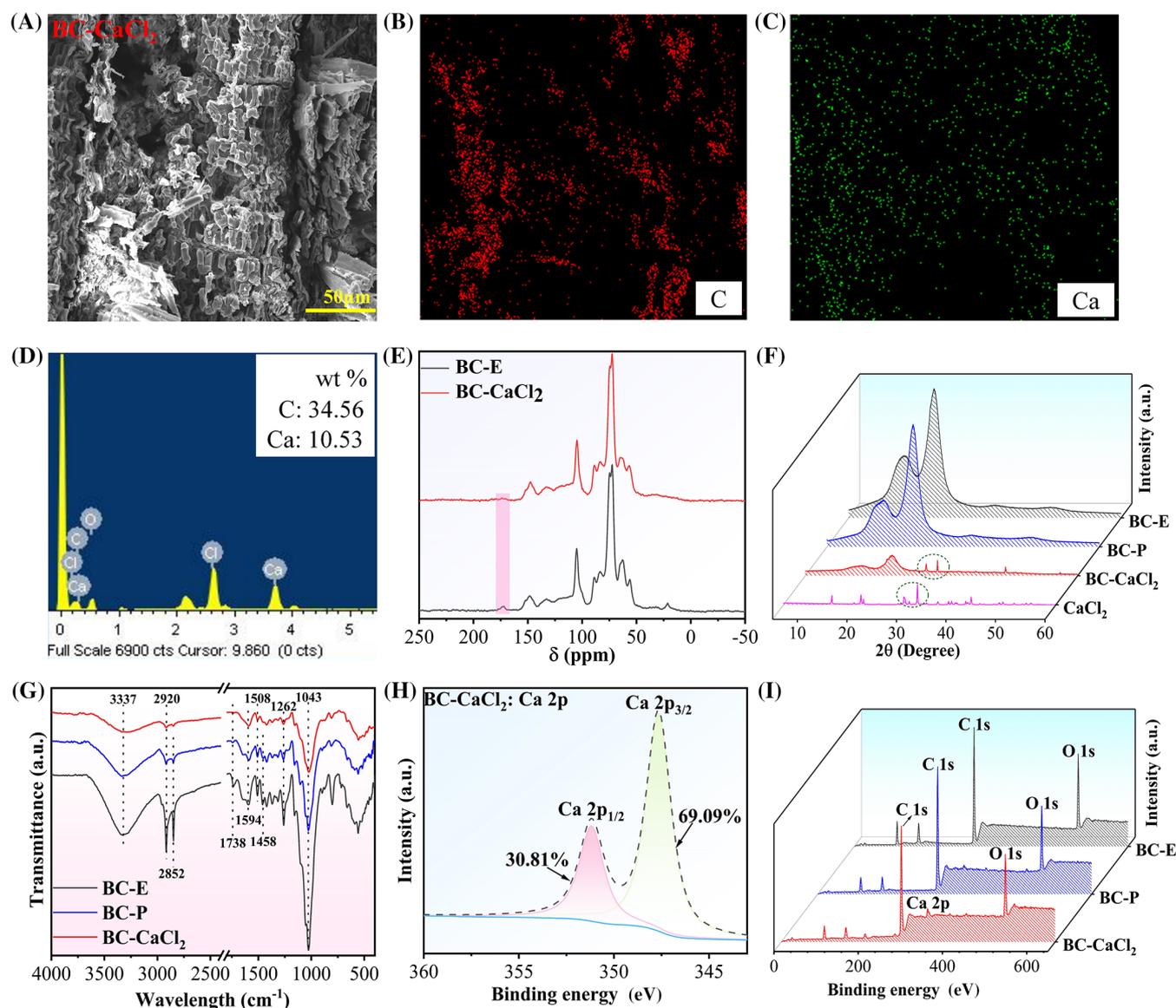

FIGURE 3   (A) Section SEM image of the fractured BC-$CaCl_2$. The mapping of elemental (B) C and (C) Ca. (D) EDS spectrum the element content in BC-$CaCl_2$. (E) Comparison of ^{13}C-NMR of BC-E and BC-$CaCl_2$ in the range of -50–250 ppm. (F) XRD patterns of BC-E, BC-P, BC-$CaCl_2$, and $CaCl_2$. (G) FT-IR and (I) XPS total spectra of BC-E, BC-P, and BC-$CaCl_2$. (H) Ca 2p XPS spectra of BC-$CaCl_2$.

−COOH in hemicellulose and Ca^{2+}.[60,61] Through ^{13}C-NMR spectrum analysis, the peak value of BC-CaCl$_2$ in hemicellulose (170–175 ppm) disappears almost completely, which is due to the coordination crosslinks between −COOH in hemicellulose and Ca^{2+}, forming a stable wood structure (Figure 3E).[62] As shown in Figure 3G, the peak of BC-CaCl$_2$ at 3337 cm^{-1} (O—H bending vibration) is significantly reduced compared to BC-E and BC-P, which indicates the reduction of free hydroxyl. The absorption peaks of lignin at 1594, 1508, and 1458 cm^{-1} (benzene ring skeleton vibration) of BC-CaCl$_2$ are consistent with those of BC-P and much lower than those of BC-E.[63,64] This is because the lignin in pinewood is partially removed under the pretreatment of alkaline solution. Meanwhile, the peak of BC-CaCl$_2$ at 1738 cm^{-1} almost completely disappeared, indicating the removal of the characteristic absorption peak (C=O stretching vibration) of hemicellulose formed by the acetyl and carboxyl groups of hemicellulose, which is consistent with ^{13}C-NMR results.[65]

In addition, the characteristic peaks of Raman spectrum in the range of 1535–1650 cm^{-1} are mainly derived from lignin (Figure S1B). The image shows that the peaks of BC-CaCl$_2$ at 1537 cm^{-1} (CH$_3$ bending in O—CH$_3$) and 1643 cm^{-1} (C=C telescopic vibration) are significantly weaker than those of BC-E, which indicates a substantial removal of lignin and is consistent with the above results.[66]

X-ray diffraction patterns show that only BC-CaCl$_2$ has a diffraction peak consistent with CaCl$_2$ in the range of diffraction angle from 30 to 40° (Figure 3F). This proves that CaCl$_2$ exists in the interior of the pretreated pinewood after vacuum impregnation, thus providing coordination conditions for the internal crosslinks of BC-CaCl$_2$. In addition, the weakening of the diffraction peaks in the BC-CaCl$_2$ crystalline and the amorphous regions are due to the structural changes caused by the addition of CaCl$_2$ crystals.

The structure composition of BC-CaCl$_2$ was determined by analyzing three peaks of C, O, and Ca in the XPS full spectrum. The structural composition of BC-CaCl$_2$ was determined by analyzing the three peaks of C, O, and Ca in the XPS full spectrum. As shown in Figure 3H,I, only the XPS spectrum of BC-CaCl$_2$ has a peak of Ca 2p, indicating the introduction of Ca^{2+} successfully formed ion bonds with −COOH in hemicellulose, and formed a high-density cross-linked structure under the interaction of hydrogen bonds, thus building a stable wood system.[67]

## 3.4 | Morphology and mechanical properties of BC-CaCl$_2$

SEM images reveal that the cross-section of BC-E is clearly layered, and the fibers are compressed and tightly connected after the cell wall collapses (Figure 4A). Hence, there are still some gaps between the fiber layers. Figure 4B shows that the internal cell structure of BC-P thermoformed after alkali treatment is destroyed, and the complete wood structure cannot be seen in the section.[68] Since part of the lignin has been removed, its internal structure is partially porous. As supported by Section 3.2, BC-CaCl$_2$ forms coordination crosslinks under the action of Ca^{2+}, and recombines the fibers under the action of intermolecular hydrogen bonds, showing a stable internal structure (Figure 4C).[69] Meanwhile, its internal structure is composed of closely connected states similar to building blocks, so there are almost no pores. In addition, BC-CaCl$_2$ becomes dense after hot pressing, reducing its thickness by more than 65% (Figure S2B). Although the mass of BC-P is reduced due to the removal of lignin, the high-density cross-linked structure formed in BC-CaCl$_2$ due to the addition of Ca^{2+} leads to a high density of 1.58 g/cm^3 (Figure S2A).

The mechanical tests show that the tensile strength of BC-CaCl$_2$ (470.5 MPa) is much higher than that of BC-E (206.7 MPa) and BC-P (263.5 MPa) (Figure 4D,F). Meanwhile, the flexural strength of BC-CaCl$_2$ (470.5 MPa) is also much higher than that of BC-E (206.7 MPa) and BC-P (263.5 MPa) (Figure 4G,I). In addition, the tensile modulus and flexural modulus of BC-CaCl$_2$ are higher than those of BC-E and BC-P (Figure 4E,H).[70] The results indicate that a stable high-density cross-linked structure is formed inside BC-CaCl$_2$, which enhances the bonding strength between fibers. This discovery is attributed to the formation of coordination crosslinks between −COOH in hemicellulose and Ca^{2+}, which enhances the internal binding of BC-CaCl$_2$ under the combined action of intermolecular hydrogen bond. On the other hand, Figure 4J shows the excellent specific strength of BC-CaCl$_2$, surpassing most typical structural materials, especially some metals and alloys.[71] In summary, the excellent mechanical properties of BC-CaCl$_2$ provide a solid foundation for its application as a structural material in the building materials industry, such as anti-seismic buildings.

3.5 | Color difference and water resistance of BC-CaCl$_2$

The color difference experiment (Figure 5A) shows that Ba-CaCl$_2$ has a lower lightness than BC-E and BC-P. This indicates that BC-CaCl$_2$ has the highest degree of surface charring.[72] This is because part of the lignin in BC-CaCl$_2$ is removed by the alkali solution, and the remaining lignin melts and overflows during the thermoforming process. However, its internal stable structure inhibits the recombination of lignin, so a dense protective layer is formed on
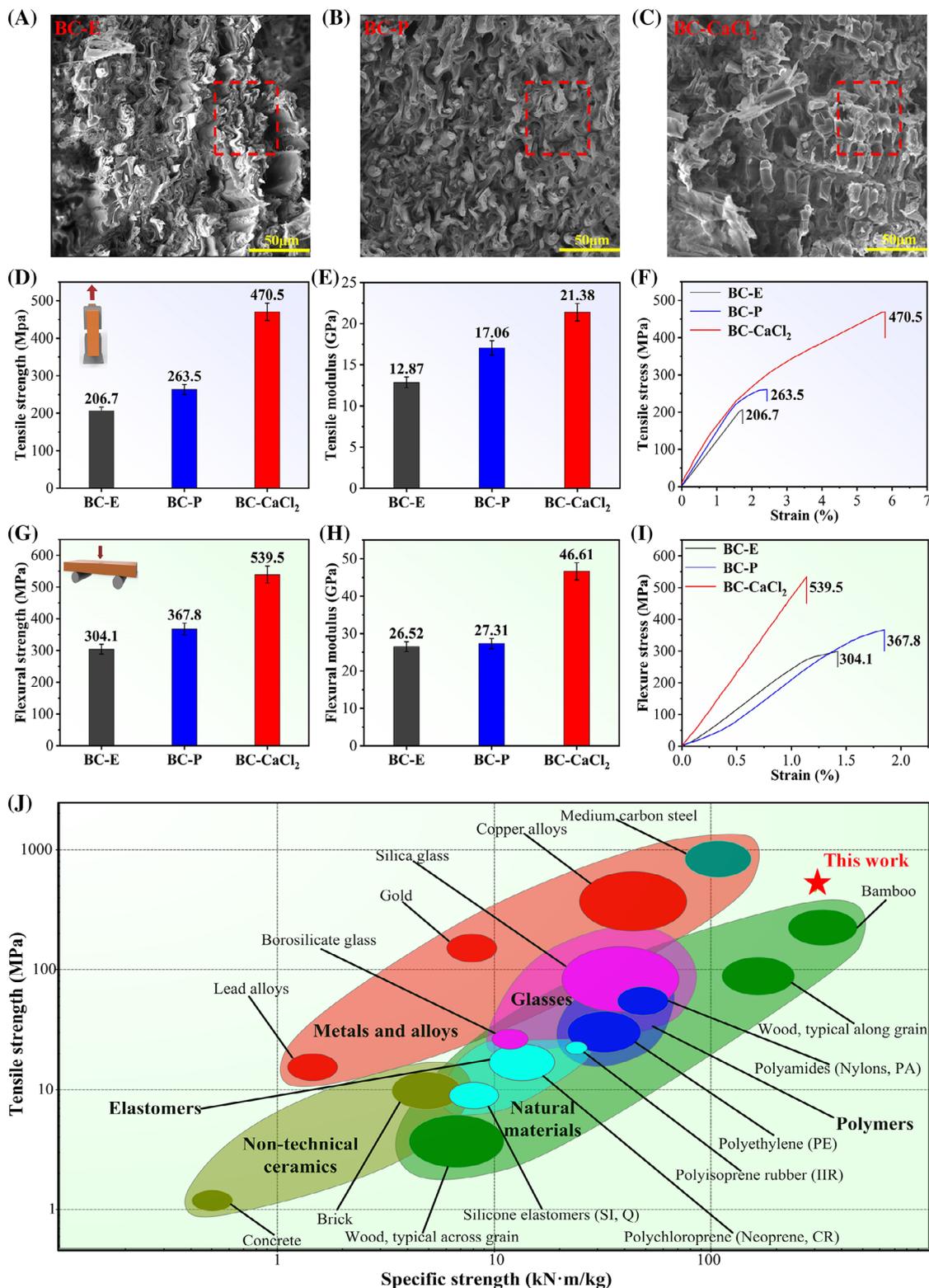
FIGURE 4 SEM images of the cross section of (A) BC-E, (B) BC-P and (C) BC-CaCl$_2$. (D) Tensile strength, (E) tensile modulus, (G) flexural strength and (H) flexural modulus of BC-E, BC-P and BC-CaCl$_2$. (F) Tensile and (I) flexural stress–strain curves of BC-E, BC-P and BC-CaCl$_2$. (J) Comparison diagram of tensile strength-specific strength between BC-CaCl$_2$ and other materials.

the surface of BC-CaCl$_2$ after cooling. The SEM observations show that the surface of BC-E and BC-P is full of cracks, while the surface of BC-CaCl$_2$ is flat and smooth,

making it difficult for moisture to enter the interior of the material (Figure S3).[73] This phenomenon is attributed to the protective layer structure formed by lignin.
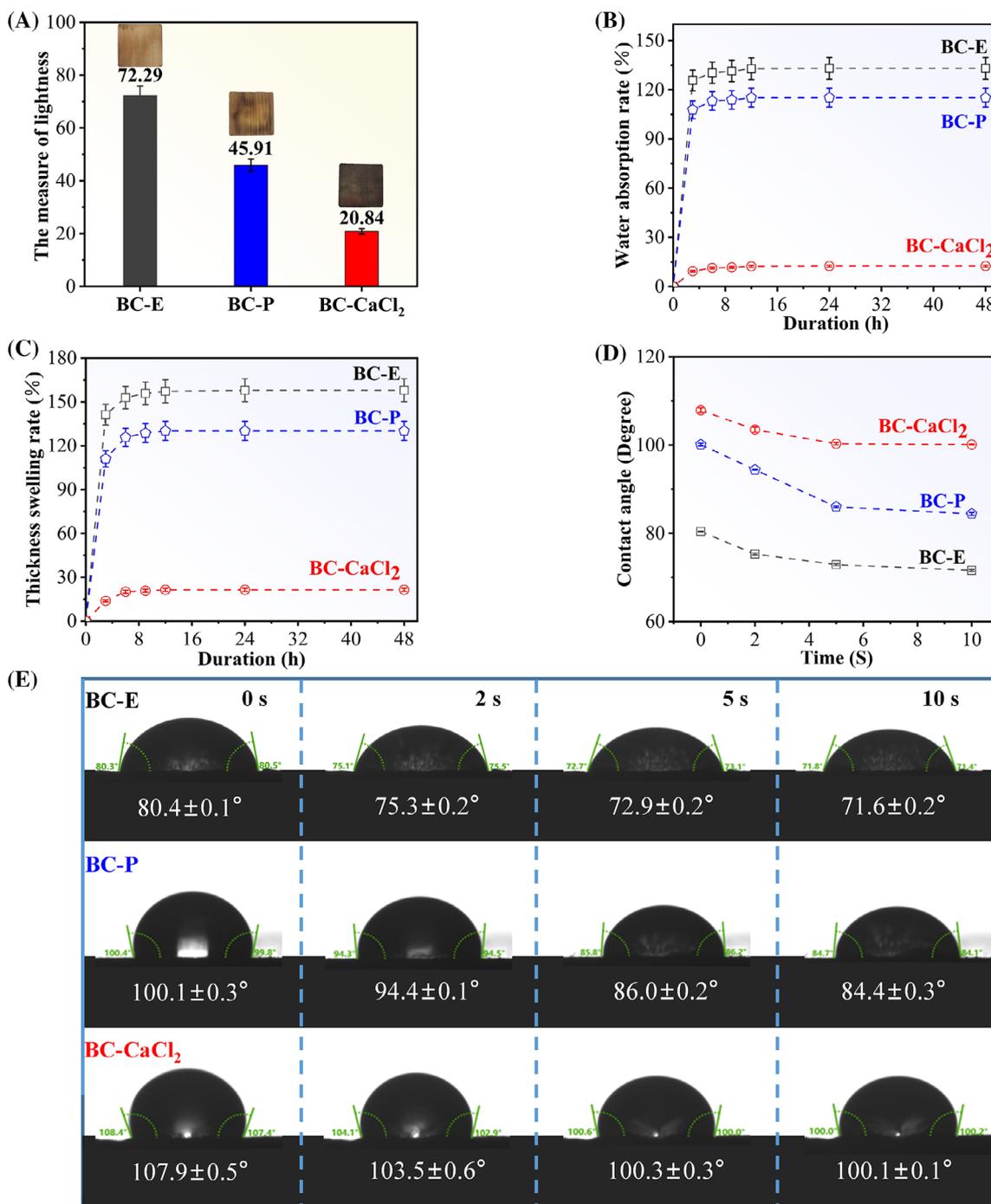
FIGURE 5 (A) Lightness comparison of BC-E, BC-P, and BC-CaCl$_2$. (B) Water absorption rate comparison of BC-E, BC-P, and BC-CaCl$_2$. (C) Water absorption thickness swelling rate comparison of BC-E, BC-P, and BC-CaCl$_2$. (D) Contact angle-time curve of BC-E, BC-P, and BC-CaCl$_2$. (E) Contact angle photographs of BC-E, BC-P, and BC-CaCl$_2$ at 0, 2, 5, and 10 s.

Furthermore, the stable building blocks structure inside BC-CaCl$_2$ also hinders the absorption of water (Figure 4C). Therefore, the water resistance test of BC-E, BC-P, and BC-CaCl$_2$ soaked in water for 2 days shows that the water absorption rate and water absorption thickness expansion rate of BC-CaCl$_2$ (12.48%, 21.38%) are much lower than those of BC-E (133.05%, 157.97%) and BC-P (115.12%, 130.15%) (Figure 5B,C).

Meanwhile, the contact angle test shows that BC-CaCl$_2$ has the highest contact angle and is stable above 100° (Figure 5D,E),[74] showing that BC-CaCl$_2$ has the best water stability. This property is attributed to the reduction of hydrophilic group −OH under the treatment conditions of alkaline solution, which corresponds to the FT-IR results (Figure 3G). Meanwhile, the protective layer formed by lignin on the surface of the materials

makes it difficult for water to penetrate. Furthermore, the high-density cross-linked structure inside BC-CaCl$_2$ can improve its dimensional stability, thereby greatly enhancing its water resistance. Hence, BC-CaCl$_2$ can be used in indoor areas with high humidity, such as toilets, bathrooms and kitchens as well as in the envelope structure of outdoor buildings to prevent the infiltration of rain, snow and groundwater.

3.6 | Thermal conductivity and thermal stability of BC-CaCl$_2$

Thermal conductivity tests show that the thermal conductivity of BC-CaCl$_2$ is higher than that of BC-E and BC-P (Figure 6A,B). Meanwhile, the infrared thermal

imaging experiment shows that the thermal diffusion degree of BC-CaCl$_2$ is the largest within the heating time of 3 min, which is consistent with the result of the highest thermal conductivity (Figure S4). This is because Ca^{2+} is a benign conductor of heat. It collides with free electrons in BC-CaCl$_2$, and the unbound free electrons move freely inside the material, which can conduct heat. Therefore, the excellent thermal conductivity makes BC-CaCl$_2$ suitable for indoor floor heating systems and heat dissipation of high-power devices such as communication in place of thermal conductive rubber.[75]

The thermal stability of BC-CaCl$_2$ and other materials is evaluated by TGA analysis (Figure 6C). Three stages of pyrolysis in air are observed, that is, dehydration, oxidative pyrolysis and carbonization stages. The thermal degradation of BC-CaCl$_2$ mainly occurs at about 230–400°C,

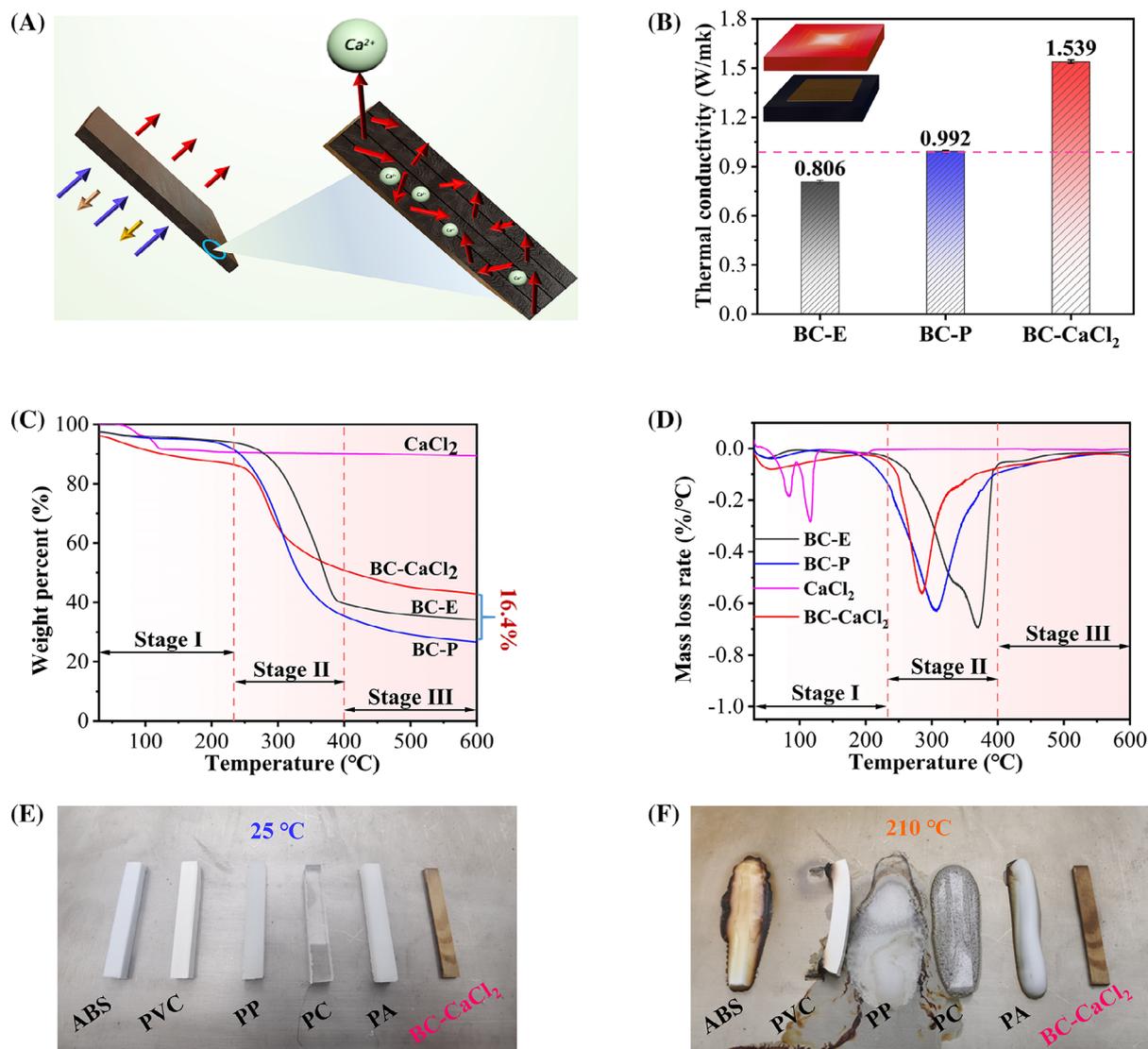**FIGURE 6** (A) Schematic diagram of thermal conductivity mechanism of BC-CaCl$_2$. (B) Thermal conductivity comparison of BC-E, BC-P, and BC-CaCl$_2$. (C) TG and (D) DTG curves of BC-E, BC-P, BC-CaCl$_2$, and CaCl$_2$. (E) Comparison diagram of thermal stability of BC-CaCl$_2$ and several normal used plastics at 25°C. (F) Comparison diagram of thermal stability of BC-CaCl$_2$ and several normal used plastics at 210°C.

which is the degradation stage of cellulose and hemicellulose. Since crystal $CaCl_2$ is not easily thermally degraded, BC-$CaCl_2$ has the lowest mass loss and the final residue is 16.4% more than that of treated BC-P. However, the maximum degradation temperature of BC-$CaCl_2$ is lower than that of BC-E and BC-P. This is due to the formation of coordination crosslinks between $-COOH$ in hemicellulose and Ca^{2+}. During the heating process, ions are not bound but move freely, making the internal structure of material unstable.

Meanwhile, the DTG curve (Figure 6D) shows that the maximum degradation rate corresponding to the maximum degradation temperature of BC-$CaCl_2$ is the lowest.[76] Moreover, the weight loss temperature of BC-$CaCl_2$ between 230 and 300°C is lower than that of BC-E and BC-P due to the decrease of lignin content. Hence, this property can be applied to develop materials with good thermal insulation properties, such as insulation materials in construction. The combustion experiment after 10 s shows that BC-E and BC-P emit strong flames and spread rapidly while BC-$CaCl_2$ is hardly ignited (Figure S5a). In addition, most of BC-E and BC-P have been charred and turned black after 10 s, while BC-$CaCl_2$ still maintains its structural integrity (Figure S5b).[77] It can be directly observed from Figure 6E,F that BC-$CaCl_2$ can maintain the initial stable shape on the heating stage at 210°C, while other commonly used plastics have all softened and deformed.[78] The above results show that BC-$CaCl_2$ has excellent thermal stability, compared to existing petrochemical plastics. This is because lignin forms a dense protective layer on the surface of BC-$CaCl_2$, which hinders the flame combustion of the material. Therefore, good thermal stability of BC-$CaCl_2$ makes it possible to replace petrochemical-based materials, such as plastics for pipes and packaging materials. It further tackles the pollution problem that waste plastics are difficult to handle from the source, which is in line with the concept of clean production.

3.7 | UV resistance, corrosion resistance and antibacterial properties of BC-$CaCl_2$

Figure 7A shows a schematic diagram of the UV resistance, corrosion resistance and antibacterial properties of BC-$CaCl_2$. BC-$CaCl_2$ absorbs almost all ultraviolet light (94%), including UVA (315–400 nm), UVB (280–315 nm), and UVC (200–280 nm) (Figure 7B). Meanwhile, the UV transmittance of BC-$CaCl_2$ is the lowest meaning that BC-$CaCl_2$ can completely shield UV radiation. This is because the surface of BC-$CaCl_2$ is covered with a protective layer composed of lignin, and the lignin molecules contain a large number of phenylpropane units with phenol hydroxyl groups, which can strongly absorb UV light. The excellent UV resistance enables BC-$CaCl_2$ to replace the UV resistant fiber for weaving outdoor products such as sunshades and outdoor UV resistant polymers.[79]

The antibacterial test after 24 h shows an obvious inhibition zone around BC-$CaCl_2$, while the rest of the samples had no obvious changes (Figure 7C, S6A).[80] The phenomenon demonstrates excellent antibacterial properties of BC-$CaCl_2$ because Ca^{2+} will affect the metabolism of microorganisms.[81,82] This makes BC-$CaCl_2$
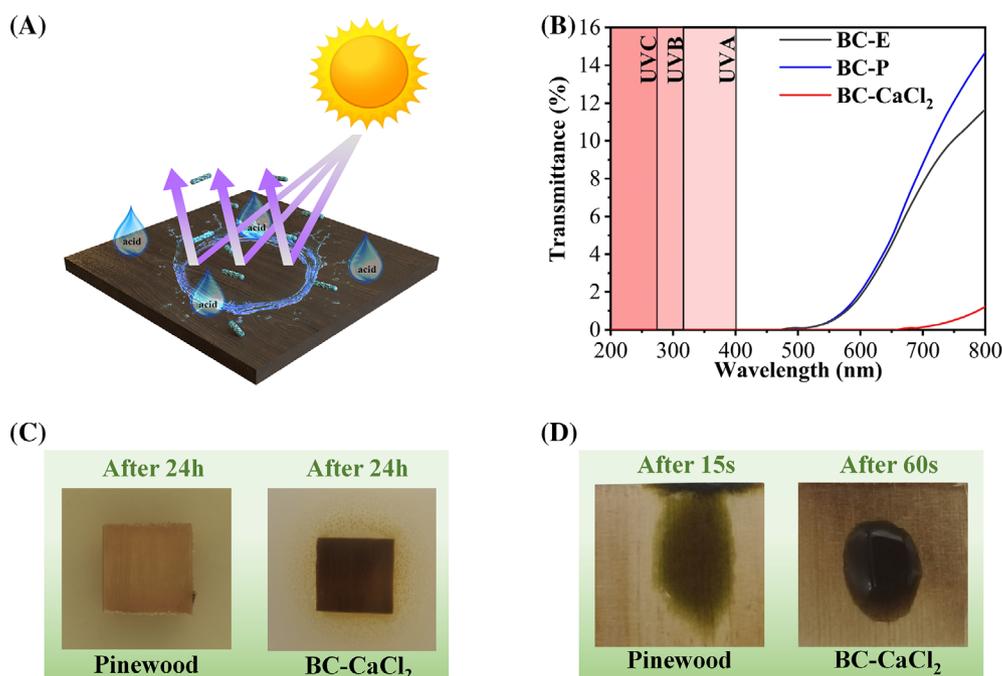
FIGURE 7 (A) Schematic diagram of UV, antibacterial and corrosion resistance of BC-$CaCl_2$. (B) UV transmittance curves of BC-E, BC-P, and BC-$CaCl_2$. (C) Comparison of antibacterial resistance between pinewood and BC-$CaCl_2$. (D) Comparison of acid resistance between pinewood and BC-$CaCl_2$.

suitable for food and pharmaceutical packaging. In addition, BC-CaCl$_2$ has a good corrosion resistance due to its excellent water resistance, which prevents sulfuric acid from entering the interior of the material (Figure 7D, S6B). Coupled with the outstanding mechanical properties of BC-CaCl$_2$, it can be used as an anti- corrosion material in comparison to stainless steel in the field of installation engineering.[83–85]

4 | CONCLUSIONS

This study develops an efficient process for facile fabrication of high-performance, sustainable wood-based structural functional materials BC-CaCl$_2$, based on natural pinewood. Ca^{2+} was used to build a high-density cross-linked structure in pinewood, including high-density hydrogen bonds between cellulose microfiber and hemicellulose, and coordination crosslinks between Ca^{2+} and −COOH. The stable internal structure endows BC-CaCl$_2$ with outstanding tensile strength (470.5 MPa) and flexural strength (539.5 MPa), providing structural advantages for the application of the material. Moreover, BC-CaCl$_2$ exhibits excellent water resistance, thermal conductivity, thermal stability, UV resistance, corrosion resistance and antibacterial properties. The prepared high-performance wood-based composites address the inefficient use of pinewood and achieve the high-value utilization of natural wood. Meanwhile, the simple preparation process of one-step thermoforming is conducive to the further development and practical application of wood-based composites in the field of structural and functional materials. The potential application areas for BC-CaCl$_2$ include waterproof enclosure structure of buildings, indoor underfloor heating, outdoor UV resistant protective cover and anti-corrosion materials for installation engineering, and so forth. The as-prepared BC-CaCl$_2$ may have the potential to replace traditional petrochemical-based materials for a wide range of applications, such as replacing plastics for pipelines and packaging materials. However, wood-based structural functional materials often require special treatment and protection to improve their performance and durability. Future research will improve the durability of the material by applying protective layers. Due to the limitations of hot-pressing technology and solid wood as raw materials, the material is also subject to processability limitations in practical applications. Hence, multiple molds can be developed in the future to suit a variety of application scenarios.

AUTHOR CONTRIBUTIONS
Haoran Ye and Yang Shi carried the experimental work and data processing, Wei Fan, Zhongfeng Zhang, Daniel M. Mulvihill and Pengju Shi helped in data analysis, Ben Bin Xu design the work program with Zhanhu Guo, Xuehua Zhang, Ximin He and Shengbo Ge. All authors contributed in the manuscript drafting.

CONFLICT OF INTEREST STATEMENT
We confirm that the work submitted is not under consideration elsewhere. Prof Ximin He is an Editorial Board member of EcoMat and a co-author of this article. To minimize bias, she should be excluded from all editorial decision-making related to the acceptance of this article for publication. Otherwise, no further conflict of interest in this submission.

ORCID
Ben Bin Xu https://orcid.org/0000-0002-6747-2016
Wei Fan https://orcid.org/0000-0001-9850-9734
Ximin He https://orcid.org/0000-0001-8845-4637

REFERENCES
1. Feng Y, Li Y, Almalki ASA, et al. Synthesis and characterization of poly(butanediol sebacate-butanediol) terephthalate (PBSeT) reinforced by hydrogen bond containing amide group, with good mechanical properties and improved water vapor barrier. *Adv Compos Hybrid Mater*. 2022;5(3):2051-2065. doi:10.1007/s42114-022-00542-y
2. Ziyadi H, Baghali M, Bagherianfar M, Mehrali F, Faridi-Majidi R. An investigation of factors affecting the electrospinning of poly (vinyl alcohol)/kefiran composite nanofibers. *Adv Compos Hybrid Mater*. 2021;4(3):768-779. doi:10.1007/s42114-021-00230-3
3. Zhu E-Q, Xu G-F, Sun S-F, et al. Rosin acid modification of bamboo powder and thermoplasticity of its products based on hydrothermal pretreatment. *Adv Compos Hybrid Mater*. 2021;4(3):584-590. doi:10.1007/s42114-021-00266-5
4. Ye H, Wang Y, Yu Q, et al. Bio-based composites fabricated from wood fibers through self-bonding technology. *Chemosphere*. 2021;287(Pt 4):132436. doi:10.1016/j.chemosphere.2021.132436

5. Ge S, Ouyang H, Ye H, Shi Y, Sheng Y, Peng W. High-performance and environmentally friendly acrylonitrile butadiene styrene/wood composite for versatile applications in furniture and construction. *Adv Compos Hybrid Mater*. 2023; 6(1):44. doi:10.1007/s42114-023-00628-1

6. Guan Q-F, Han Z-M, Yang H-B, Ling Z-C, Yu S-H. Regenerated isotropic wood. *Natl Sci Rev*. 2020;8(7):nwaa230. doi:10.1093/nsr/nwaa230

7. Sánchez C. Fungal potential for the degradation of petroleum-based polymers: An overview of macro- and microplastics biodegradation. *Biotechnol Adv*. 2020;40:107501. doi:10.1016/j.biotechadv.2019.107501

8. Meng X, Yang H, Lu Z, Liu Y. Study on catalytic pyrolysis and combustion characteristics of waste cable sheath with cross-linked polyethylene. *Adv Compos Hybrid Mater*. 2022;5(4): 2948-2963. doi:10.1007/s42114-022-00516-0

9. Meereboer KW, Misra M, Mohanty AK. Review of recent advances in the biodegradability of polyhydroxyalkanoate (PHA) bioplastics and their composites. *Green Chem*. 2020; 22(17):5519-5558. doi:10.1039/D0GC01647K

10. Zhang H, Zhong J, Liu Z, Mai J, Liu H, Mai X. Dyed bamboo composite materials with excellent anti-microbial corrosion. *Adv Compos Hybrid Mater*. 2021;4(2):294-305. doi:10.1007/s42114-020-00196-8

11. Tian J, Yu L, Xue R, Zhuang S, Shan Y. Global low-carbon energy transition in the post-COVID-19 era. *Appl Energy*. 2022; 307:118205. doi:10.1016/j.apenergy.2021.118205

12. Yuan B, Wang Y, Elnaggar AY, et al. Physical vapor deposition of graphitic carbon nitride (g-C3N4) films on biomass substrate: optoelectronic performance evaluation and life cycle assessment. *Adv Compos Hybrid Mater*. 2022;5(2):813-822. doi:10.1007/s42114-022-00505-3

13. Culebras M, Collins GA, Beaucamp A, Geaney H, Collins MN. Lignin/Si hybrid carbon nanofibers towards highly efficient sustainable Li-ion anode materials. *Eng Sci*. 2022;17:195-203. doi:10.30919/es8d608

14. Mu L, Dong Y, Li L, Gu X, Shi Y. Achieving high value utilization of bio-oil from lignin targeting for advanced lubrication. *ES Mater Manuf*. 2021;11:72-80. doi:10.30919/esmm5f1146

15. Xu J, Zhu P, El Azab IH, et al. An efficient bifunctional Ni-Nb2O5 nanocatalysts for the hydrodeoxygenation of anisole. *Chin J Chem Eng*. 2022;49:187-197. doi:10.1016/j.cjche.2022.07.009

16. Vinod A, Sanjay MR, Suchart S, Jyotishkumar P. Renewable and sustainable biobased materials: An assessment on biofibers, biofilms, biopolymers and biocomposites. *J Clean Prod*. 2020;258:120978. doi:10.1016/j.jclepro.2020.120978

17. Al-Tayyar NA, Youssef AM, Al-hindi R. Antimicrobial food packaging based on sustainable bio-based materials for reducing foodborne pathogens: a review. *Food Chem*. 2020;310: 125915. doi:10.1016/j.foodchem.2019.125915

18. Xiao S, Chen C, Xia Q, et al. Lightweight, strong, moldable wood via cell wall engineering as a sustainable structural material. *Science*. 2021;374(6566):465-471. doi:10.1126/science.abg9556

19. Sun Z, Zhang Y, Guo S, et al. Confining FeNi nanoparticles in biomass-derived carbon for effectively photo-Fenton catalytic reaction for polluted water treatment. *Adv Compos Hybrid Mater*. 2022;5(2):1566-1581. doi:10.1007/s42114-022-00477-4

20. Wei D, Weng M, Mahmoud MHH, et al. Development of novel biomass hybrid aerogel supported composite phase change materials with improved light-thermal conversion and thermal energy storage capacity. *Adv Compos Hybrid Mater*. 2022;5(3): 1910-1921. doi:10.1007/s42114-022-00519-x

21. Chen W, Lin H, Wu Y, et al. Fluorescent probe of nitrogen-doped carbon dots derived from biomass for the sensing of MnO4− in polluted water based on inner filter effect. *Adv Compos Hybrid Mater*. 2022;5(3):2378-2386. doi:10.1007/s42114-022-00443-0

22. Qi G, Liu Y, Chen L, et al. Lightweight Fe3C@Fe/C nanocomposites derived from wasted cornstalks with high-efficiency microwave absorption and ultrathin thickness. *Adv Compos Hybrid Mater*. 2021;4(4):1226-1238. doi:10.1007/s42114-021-00368-0

23. Deng Z, Deng Q, Wang L, et al. Modifying coconut shell activated carbon for improved purification of benzene from volatile organic waste gas. *Adv Compos Hybrid Mater*. 2021;4(3):751-760. doi:10.1007/s42114-021-00273-6

24. Gao T, Ma Y, Ji L, et al. Nickel-coated wood-derived porous carbon (Ni/WPC) for efficient electromagnetic interference shielding. *Adv Compos Hybrid Mater*. 2022;5(3):2328-2338. doi:10.1007/s42114-022-00420-7

25. Ong HC, Chen W-H, Singh Y, Gan YY, Chen C-Y, Show PL. A state-of-the-art review on thermochemical conversion of biomass for biofuel production: a TG-FTIR approach. *Energ Conver Manage*. 2020;209:112634. doi:10.1016/j.enconman.2020.112634

26. Ge S, Shi Y, Chen X, et al. Sustainable upcycling of plastic waste and wood fibers into high-performance laminated wood-polymer composite via one-step cell collapse and chemical bonding approach. *Adv Compos Hybrid Mater*. 2023;6(4):146. doi:10.1007/s42114-023-00723-3

27. Ge S, Liang Y, Zhou C, et al. The potential of Pinus armandii Franch for high-grade resource utilization. *Biomass Bioenergy*. 2022;158:106345. doi:10.1016/j.biombioe.2022.106345

28. Naik V, Kumar M, Kaup V. A review on natural fiber composite material in automotive applications. *Eng Sci*. 2022;18:1-10.

29. Pai A, Kini AK, Kini CR, Satish Shenoy B. Effect of natural fibre-epoxy plies on the mechanical and shock wave impact response of fibre metal laminates. *Eng Sci*. 2022;19: 292-300.

30. Scaffaro R, Maio A, Gammino M. Hybrid biocomposites based on polylactic acid and natural fillers from Chamaerops humilis dwarf palm and Posidonia oceanica leaves. *Adv Compos Hybrid Mater*. 2022;5(3):1988-2001. doi:10.1007/s42114-022-00534-y

31. Ge S, Ma NL, Jiang S, et al. Processed bamboo as a novel formaldehyde-free high-performance furniture biocomposite. *ACS Appl Mater Interfaces*. 2020;12(27):30824-30832. doi:10.1021/acsami.0c07448

32. Duan X, Cheng S, Tao R, Zhang Z, Zhao G. Synergistically enhanced thermal control ability and mechanical properties of natural rubber for tires through a graphene/silica with a dot-face structure. *Adv Compos Hybrid Mater*. 2022;5(2):1145-1157. doi:10.1007/s42114-022-00453-y

33. Chen C, Hu J, Xu Z, et al. Natural methionine-passivated MAPbI3 perovskite films for efficient and stable solar devices. *Adv Compos Hybrid Mater*. 2021;4(4):1261-1269. doi:10.1007/s42114-021-00238-9

34. Ge S, Chen X, Li D, et al. Hemicellulose structural changes during steam pretreatment and biogradation of Lentinus edodes. *Arab J Chem*. 2018;11(6):771-781. doi:10.1016/j.arabjc.2017.12.022

35. Liu T-T, Cao M-Q, Fang Y-S, Zhu Y-H, Cao M-S. Green building materials lit up by electromagnetic absorption function: a review. *J Mater Sci Technol*. 2022;112:329-344. doi:10.1016/j.jmst.2021.10.022

36. Fan M, Wu L, Hu Y, et al. A highly stretchable natural rubber/buckypaper/natural rubber (NR/N-BP/NR) sandwich strain sensor with ultrahigh sensitivity. *Adv Compos Hybrid Mater*. 2021;4(4):1039-1047. doi:10.1007/s42114-021-00298-x

37. Yan J, Niu Y, Wu C, et al. Antifungal effect of seven essential oils on bamboo. *Adv Compos Hybrid Mater*. 2021;4(3):552-561. doi:10.1007/s42114-021-00251-y

38. Mai X, Mai J, Liu H, et al. Advanced bamboo composite materials with high-efficiency and long-term anti-microbial fouling performance. *Adv Compos Hybrid Mater*. 2022;5(2):864-871. doi:10.1007/s42114-021-00380-4

39. Zhu E-Q, Xu G-F, Ye X-Y, et al. Preparation and characterization of hydrothermally pretreated bamboo powder with improved thermoplasticity by propargyl bromide modification in a heterogeneous system. *Adv Compos Hybrid Mater*. 2021;4(4):1059-1069. doi:10.1007/s42114-021-00316-y

40. Ji M, Li J, Li F, et al. A biodegradable chitosan-based composite film reinforced by ramie fibre and lignin for food packaging. *Carbohydr Polym*. 2022;281:119078. doi:10.1016/j.carbpol.2021.119078

41. Eisen A, Bussa M, Roeder H. A review of environmental assessments of biobased against petrochemical adhesives. *J Clean Prod*. 2020;277:277. doi:10.1016/j.jclepro.2020.124277

42. Mittal N, Janson R, Widhe M, et al. Ultrastrong and bioactive nanostructured bio-based composites. *ACS Nano*. 2017;11(5):5148-5159. doi:10.1021/acsnano.7b02305

43. Chen C, Kuang Y, Zhu S, et al. Structure-property-function relationships of natural and engineered wood. *Nat Rev Mater*. 2020;5(9):642-666. doi:10.1038/s41578-020-0195-z

44. Liang C, Du Y, Wang Y, Ma A, Huang S, Ma Z. Intumescent fire-retardant coatings for ancient wooden architectures with ideal electromagnetic interference shielding. *Adv Compos Hybrid Mater*. 2021;4(4):979-988. doi:10.1007/s42114-021-00274-5

45. Yuan B, Guo M, Murugadoss V, Song G, Guo Z. Immobilization of graphitic carbon nitride on wood surface via chemical crosslinking method for UV resistance and self-cleaning. *Adv Compos Hybrid Mater*. 2021;4(2):286-293. doi:10.1007/s42114-021-00235-y

46. Sun X, He M, Li Z. Novel engineered wood and bamboo composites for structural applications: state-of-art of manufacturing technology and mechanical performance evaluation. *Construct Build Mater*. 2020;249:118751. doi:10.1016/j.conbuildmat.2020.118751

47. Xue Y, Guo Y, Zhang X, et al. Efficient adsorptive removal of ciprofloxacin and carbamazepine using modified pinewood biochar – a kinetic, mechanistic study. *Chem Eng J*. 2022;450:137896. doi:10.1016/j.cej.2022.137896

48. Burra KG, Gupta AK. Kinetics of synergistic effects in co-pyrolysis of biomass with plastic wastes. *Appl Energy*. 2018;220:408-418. doi:10.1016/j.apenergy.2018.03.117

49. Frey M, Widner D, Segmehl JS, Casdorff K, Keplinger T, Burgert I. Delignified and densified cellulose bulk materials with excellent tensile properties for sustainable engineering. *ACS Appl Mater Interfaces*. 2018;10(5):5030-5037. doi:10.1021/acsami.7b18646

50. Guan Q-F, Yang H-B, Han Z-M, et al. Plant cellulose nanofiber-derived structural material with high-density reversible interaction networks for plastic substitute. *Nano Lett*. 2021;21(21):8999-9004. doi:10.1021/acs.nanolett.1c02315

51. Guan Q-F, Han Z-M, Yang K-P, et al. Sustainable double-network structural materials for electromagnetic shielding. *Nano Lett*. 2021;21(6):2532-2537. doi:10.1021/acs.nanolett.0c05081

52. Wang Q, Xiao S, Shi SQ, Cai L. Mechanical property enhancement of self-bonded natural fiber material via controlling cell wall plasticity and structure. *Mater Des*. 2019;172:107763. doi:10.1016/j.matdes.2019.107763

53. Luo J, Huang K, Zhou X, Xu Y. Preparation of highly flexible and sustainable lignin-rich nanocellulose film containing xylonic acid (XA), and its application as an antibacterial agent. *Int J Biol Macromol*. 2020;163:1565-1571. doi:10.1016/j.ijbiomac.2020.07.281

54. Song JW, Chen CJ, Zhu SZ, et al. Processing bulk natural wood into a high-performance structural material. *Nature*. 2018;554(7691):224-228. doi:10.1038/nature25476

55. Akpan EI, Wetzel B, Friedrich K. Eco-friendly and sustainable processing of wood-based materials. *Green Chem*. 2021;23(6):2198-2232. doi:10.1039/D0GC04430J

56. Chen B, Leiste UH, Fourney WL, Liu Y, Chen Q, Li T. Hardened wood as a renewable alternative to steel and plastic. *Matter*. 2021;4(12):3941-3952. doi:10.1016/j.matt.2021.09.020

57. Li ZH, Chen CJ, Mi RY, et al. A strong, tough, and scalable structural material from fast-growing bamboo. *Adv Mater*. 2020;32(10):1906308. doi:10.1002/adma.201906308

58. Tu K, Puértolas B, Adobes-Vidal M, et al. Green synthesis of hierarchical metal–organic framework/wood functional composites with superior mechanical properties. *Adv Sci*. 2020;7(7):1902897. doi:10.1002/advs.201902897

59. Xia QQ, Chen CJ, Yao YG, et al. A strong, biodegradable and recyclable lignocellulosic bioplastic. *Nat Sustain*. 2021;4(7):627-635. doi:10.1038/s41893-021-00702-w

60. Dai Z, Guo J, Su T, Wang J, Gao Z, Song Y-Y. Nature-inspired mineralization of a wood membrane as a sensitive electrochemical sensing device for in situ recognition of chiral molecules. *Green Chem*. 2021;23(21):8685-8693. doi:10.1039/D1GC02745J

61. Zuo S, Shi J, Wu Y, et al. Low carbon footprint preparation of MXene incorporated lignocellulosic fibers for high thermal conductivity applications. *Environ Res*. 2022;215(Pt 1):114213. doi:10.1016/j.envres.2022.114213

62. Lin Q, Huang Y, Yu W. Effects of extraction methods on morphology, structure and properties of bamboo cellulose. *Ind Crops Prod*. 2021;169:113640. doi:10.1016/j.indcrop.2021.113640

63. Li ZH, Chen CJ, Xie H, et al. Sustainable high-strength macrofibres extracted from natural bamboo. *Nat Sustain*. 2022;5(3):235-244.

64. Boonsuk P, Sukolrat A, Bourkaew S, et al. Structure-properties relationships in alkaline treated rice husk

reinforced thermoplastic cassava starch biocomposites. *Int J Biol Macromol*. 2021;167:130-140. doi:10.1016/j.ijbiomac.2020. 11.157

65. Liu Y, Coppens M-O. Cell membrane-inspired graphene Nano-mesh membrane for fast separation of oil-in-water emulsions. *Adv Funct Mater*. 2022;32(31):2200199. doi:10.1002/adfm.202200199

66. Foster EJ, Moon RJ, Agarwal UP, et al. Current characterization methods for cellulose nanomaterials. *Chem Soc Rev*. 2018;47(8):2609-2679. doi:10.1039/C6CS00895J

67. Chen J, Zhu Z, Zhang H, Tian S, Fu S. Wood-derived nanostructured hybrid for efficient flame retarding and electromagnetic shielding. *Mater Des*. 2021;204:109695. doi:10.1016/j.matdes.2021.109695

68. Montanari C, Olsen P, Berglund LA. Interface tailoring by a versatile functionalization platform for nanostructured wood biocomposites. *Green Chem*. 2020;22(22):8012-8023. doi:10.1039/D0GC02768E

69. Wang J, Chen W, Dong T, Wang H, Si S, Li X. Enabled cellulose nanopaper with outstanding water stability and wet strength via activated residual lignin as a reinforcement. *Green Chem*. 2021;23(24):10062-10070. doi:10.1039/D1GC03906G

70. Che X, Wu M, Yu G, et al. Bio-inspired water resistant and fast multi-responsive Janus actuator assembled by cellulose nanopaper and graphene with lignin adhesion. *Chem Eng J*. 2022;433:133672.

71. Chen Y, Dang B, Jin C, Sun Q. Processing lignocellulose-based composites into an Ultrastrong structural material. *ACS Nano*. 2019;13(1):371-376. doi:10.1021/acsnano.8b06409

72. Souza AG, Ferreira RR, Paula LC, Mitra SK, Rosa DS. Starch-based films enriched with nanocellulose-stabilized Pickering emulsions containing different essential oils for possible applications in food packaging. *Food Packag Shelf Life*. 2021;27:100615. doi:10.1016/j.fpsl.2020.100615

73. Zhang K, Liu Y, Guo Z, et al. Co-modification of corn straw lignin and its enhancement on glue-free fiberboard based on freezing activated wood fibers. *Ind Crops Prod*. 2022;177:114452. doi:10.1016/j.indcrop.2021.114452

74. Yang W, Pan M, Zhang J, et al. A universal strategy for constructing robust and antifouling cellulose nanocrystal coating. *Adv Funct Mater*. 2022;32(8):2109989. doi:10.1002/adfm.202109989

75. Feng X, Wang X, Wang M, Tao S, Chen Y, Qi H. High-performance carbon nanotube-cellulose nanofiber bulk materials with multifunctional applications in thermal management and shielding from electromagnetic interference. *J Mater Chem A*. 2022;10(41):22271-22277. doi:10.1039/D2TA05457D

76. Fan Q, Ou R, Hao X, et al. Water-induced self-assembly and in situ mineralization within plant phenolic glycol-gel toward Ultrastrong and multifunctional thermal insulating aerogels. *ACS Nano*. 2022;16(6):9062-9076. doi:10.1021/acsnano.2c00755

77. Hu D, Liu H, Ding Y, Ma W. Synergetic integration of thermal conductivity and flame resistance in nacre-like nanocellulose composites. *Carbohydr Polym*. 2021;264:118058. doi:10.1016/j.carbpol.2021.118058

78. Li D-H, Han Z-M, He Q, et al. Edible, ultra-strong, and thermal-stable seaweed-based structural material for tableware. *Adv Mater*. 2022;e2208098.

79. Jiang B, Chen CJ, Liang ZQ, et al. Lignin as a wood-inspired binder enabled strong, water stable, and biodegradable paper for plastic replacement. *Adv Funct Mater*. 2020;30(4):1906307. doi:10.1002/adfm.201906307

80. Ulu A, Birhanli E, Ates B. Tunable and tough porous chitosan/beta-cyclodextrin/tannic acid biocomposite membrane with mechanic, antioxidant, and antimicrobial properties. *Int J Biol Macromol*. 2021;188:696-707. doi:10.1016/j.ijbiomac.2021.08.068

81. Abral H, Kurniawan A, Rahmadiawan D, Handayani D, Sugiarti E, Muslimin AN. Highly antimicrobial and strong cellulose-based biocomposite film prepared with bacterial cellulose powders, Uncaria gambir, and ultrasonication treatment. *Int J Biol Macromol*. 2022;208:88-96. doi:10.1016/j.ijbiomac.2022.02.154

82. Tarique J, Sapuan SM, Khalina A, Ilyas RA, Zainudin ES. Thermal, flammability, and antimicrobial properties of arrowroot (Maranta arundinacea) fiber reinforced arrowroot starch biopolymer composites for food packaging applications. *Int J Biol Macromol*. 2022;213:1-10. doi:10.1016/j.ijbiomac.2022.05.104

83. Cai J, Murugadoss V, Jiang J, et al. Waterborne polyurethane and its nanocomposites: a mini-review for anti-corrosion coating, flame retardancy, and biomedical applications. *Adv Compos Hybrid Mater*. 2022;5(2):641-650. doi:10.1007/s42114-022-00473-8

84. Yan Z, Wang S, Bi J, et al. Strengthening waterborne acrylic resin modified with trimethylolpropane triacrylate and compositing with carbon nanotubes for enhanced anticorrosion. *Adv Compos Hybrid Mater*. 2022;5(3):2116-2130. doi:10.1007/s42114-022-00554-8

85. Zhu Q, Zhao Y, Miao B, et al. Hydrothermally synthesized ZnO-RGO-PPy for water-borne epoxy nanocomposite coating with anticorrosive reinforcement. *Prog Org Coat*. 2022;172:107153. doi:10.1016/j.porgcoat.2022.107153

SUPPORTING INFORMATION
Additional supporting information can be found online in the Supporting Information section at the end of this article.